Proceedings of the Institute of Acoustics

DOUBLE REED SOUND PRODUCTION ON THE BASS CRUMHORN

M. G. Aragó Bishop MPhys student, University of Edinburgh, United Kingdom
M. Campbell Senior Honorary Professorial Fellow, University of Edinburgh, United Kingdom
A. Woolley Honorary Fellow, University of Edinburgh, United Kingdom

1 INTRODUCTION

1.1 Reed Woodwind Instruments: The Crumhorn

Reed woodwind instruments are composed of a tube, considerably longer than its widest diameter, with a single or double reed at one end.[1] Double reed instruments have been less extensively studied than single reed instruments. This gap was notably addressed by André Almeida's thesis and subsequent studies, making use of artificial blowing machines and high-speed photography to investigate modern double reeds.[2,3] This paper extends such efforts by focusing on the transient behaviour of the reed in a historical instrument: the bass crumhorn.

The aim of this project is to artificially blow the crumhorn and compare its behaviour with that of a human-played crumhorn and with theoretical predictions based on a simplified model. One key benefit of the crumhorn is its cylindrical bore along most of its length, with only a short flare at the end. This design minimises the complexities typically introduced by tapered bores and bells, which can affect sound wave behaviour and resonance. By avoiding these complexities, the crumhorn's design allows for a more straightforward comparison with a theoretical model that assumes a cylindrical geometry. A further advantage of the crumhorn is its windcap, which completely encloses the reed, ensuring the player's lips do not contact the reed directly, unlike other modern double reed instruments such as the bassoon or the oboe. This feature makes the crumhorn an excellent candidate for mimicking actual musical performances through artificial blowing. In addition, this unusual instrument has already been studied in experiments on period doubling.[4]

1.2 The Double Reed

Double reeds are constructed from two bound blades of *Arundo Donax*, a plant related to bamboo. These reeds form a channel through which air is driven, causing the blades to vibrate and produce sound as the air pressure fluctuates between them. In modern double reed instruments like the oboe and bassoon, players press their lips against the reed, filtering high frequencies and producing a mellow tone. In contrast, the crumhorn's design results in a brighter, more strident timbre.

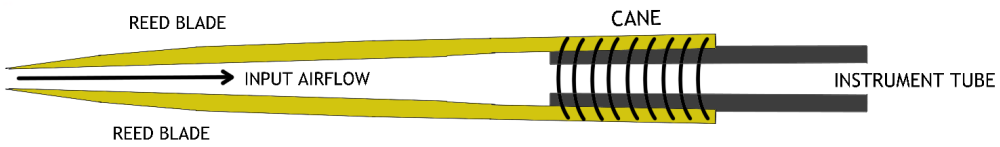

Figure 1: Simplified double reed diagram

When played with an instrument, the reed vibrates periodically at a specific frequency, modulating the airflow into the instrument at that frequency. However, this modulation is not sinusoidal, which means

the airflow contains not only the fundamental frequency of the reed but also multiple harmonics of that frequency. These harmonics generated by the reed's vibration are different from the acoustic modes of the instrument bore. The balance between the reed's natural frequency and the instrument's resonances is what allows the instrument to produce stable and controlled notes across its range. Furthermore, this cooperative regime is what allows the player to change the resulting sound of the instrument by adjusting their embouchure and blowing pressure, which effectively changes the harmonic components of the internal pressure. When the harmonics of the reed's vibration closely align with the instrument's acoustic resonance frequencies, a strong and stable note is produced.

Physical models based on non-linear dynamics have been developed to describe the physics of the double reed. The reed resonator is usually modelled as a one degree of freedom oscillator with boundary conditions that give the resonance properties of the bore.[3] This description was first introduced in 1963 by J. Backus under the study of single reed vibrations with the clarinet.[5]

This paper aims to analyse the transient behaviour of the reed with varying input pressure in the crumhorn. By replacing the normal windcap with a cylindrical Perspex cap, various playing regimes were examined under continuous stable blowing. As the blowing pressure is reduced, the instrument exhibits a number of stable playing states. To capture these states, pressure sensors are used to measure the air pressure in the windcap and mouthpiece, and reed oscillations are tracked with a laser distance sensor. A small window is fitted through which the reed opening could be observed with high-speed video recordings. This setup allows the high-speed camera to measure small rapid oscillations related to the natural frequency of the reed.

2 EQUIPMENT

This paper's data acquisition setup is based on measuring the reed height, the sound emitted from the crumhorn and the upstream and downstream pressures. The equipment setup, along with the crumhorn, is shown below in Figure 2.

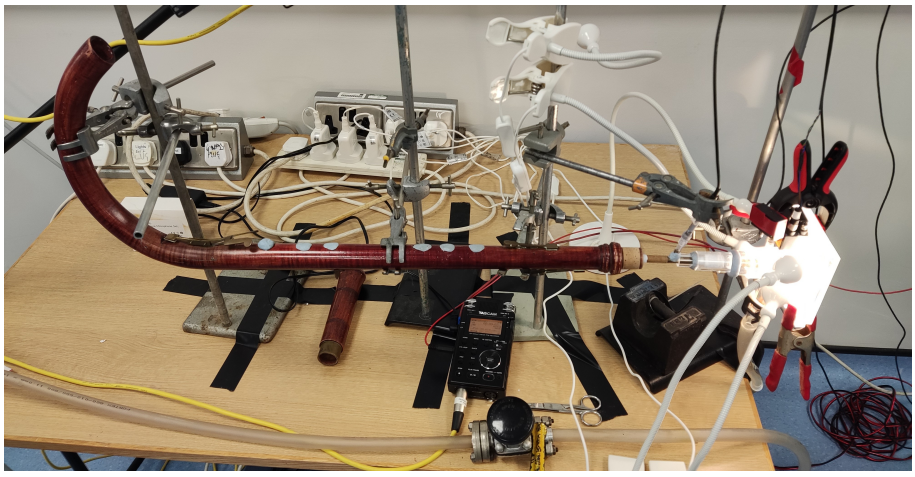

Figure 2: Mounting arrangement of the bass crumhorn, with all tone holes covered with Blutack and the 7th with its key closed.

The bass crumhorn is mounted on four metal stands, levelling the crumhorn with the camera. The instrument has six tone holes, which function by allowing the player to change the pitch by opening and closing them, thereby effectively shortening or lengthening the air column inside the bore. These tone holes are all covered with Blutack. Additionally, the crumhorn features a seventh tone hole actioned by a key, which is also kept closed. This setup ensures that the lowest nominal pitch is played when air is driven through the instrument. The windcap is replaced by a cylindrical Perspex cap, pressurised

by a multistage centrifugal air pump. A transparent acrylic window is placed parallel to the horizontal axes of the reed opening through which images of the reed are taken, as shown in Figure 3. The laser sensor is placed above the windcap, which encloses the upstream and downstream pressure sensors.

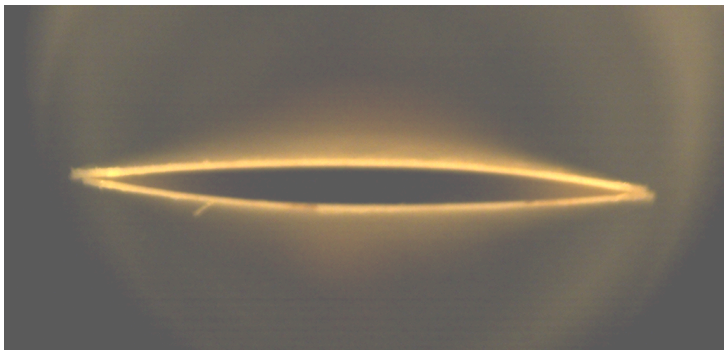

Figure 3: Double reed image viewed through the small transparent window at the reed's tip. The brightness and contrast have been adjusted to improve visibility.

The displacement of the reed is recorded with a *Baumer* OADM 12U6430/S35A laser sensor pointing at the upper blade tip of the reed. The sensor's operating range is 16 to 26 mm, with a 5 μm resolution. The upstream pressure, the pressure in the interior of the windcap, is measured with a *Sensortechnics* HCXM050D6V pressure sensor. The sensor has a pressure limit of 10 kPa, which is not exceeded by the measurent range from 0 to 5 kPa. The downstream pressure inside the reed is taken at the mouthpiece through a short tube. Readings are taken with a *G.R.A.S.* 46 BG high-pressure microphone, with a calibrated output of 0.27 mV/Pa. The signal is filtered through a PCB model 480C02 sensor signal conditioner.

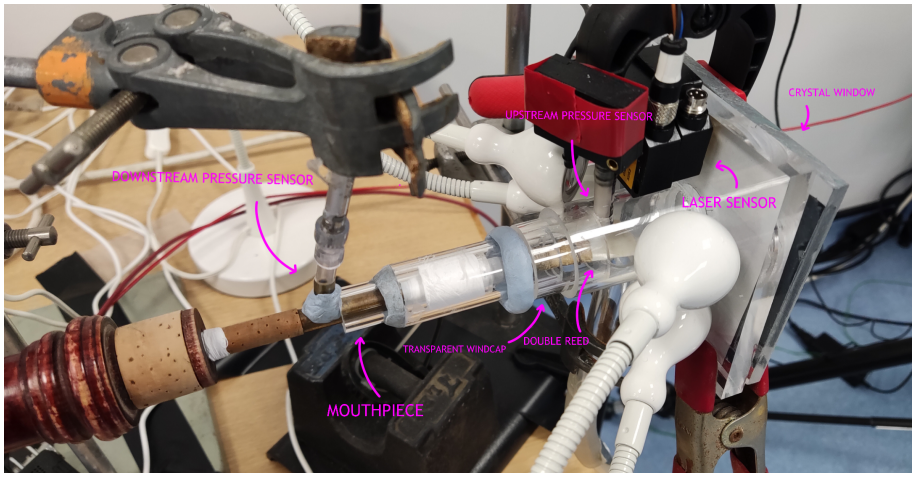

Figure 4: Transparent windcap setup with pressure and laser sensors.

The data acquisition system is an *Iotech Wavebook* 516E, with a 16-bit resolution and a maximum sampling rate of 1 MHz across all eight channels. However, due to the response time of the sensors a sampling rate of 10kHz per channel was chosen. The software used is *Waveview* version 7.15.19. The pressure and laser sensors are connected to the data acquisition system through a small signal adaptor box. Each sensor is linked to an independent channel, from which the system reads voltage. An *AKG* CE391B microphone is connected to the data acquisition system for sound recordings and also linked to a *TASCAM* DR 100 mk2 digital recorder, allowing for simultaneous recording at a higher quality. The microphone is positioned at the short flare end of the crumhorn.

A *Photron* SA 1.1 camera produces high-speed video recordings of the double reed oscillation. To achieve optimal focusing on the image (Figure 3), a Tamron Macro 80-200mm lens and extension tubes of 2.5 cm are used. In addition, LED lights are placed above and below the reed blades to highlight the image's reed shape. The software used with the camera is the *Photron Fastcam Viewer* version 3670. A manual trigger is connected to the camera and the data acquisition system to synchronise both measurements.

3 EXPERIMENTAL WORK

3.1 Measurement Procedure

Four tests were performed by measuring the behaviour of the reed height and upstream and downstream pressures with varying blowing pressure. A data-driven pitch tracking algorithm, *CREPE*, was used to obtain the sound pitch from these measurements, based on a deep convolutional neural network that operates directly on the time-domain waveform.[6] The blowing pressure serves as the varying parameter, leading to period multiplication bifurcations, where the system's oscillatory period increases by integer multiples due to its non-linear behaviour.

The first test was concerned on mimicking usual musical performances on wind instruments, where the player raises the blowing pressure and then keeps it steady during the note. This involved measuring the stability of the nominal pitch of the crumhorn with all tone holes closed (F2, 87 Hz) at a constant blowing pressure. This state is considered in the analysis as state A. The following waveforms are observed,

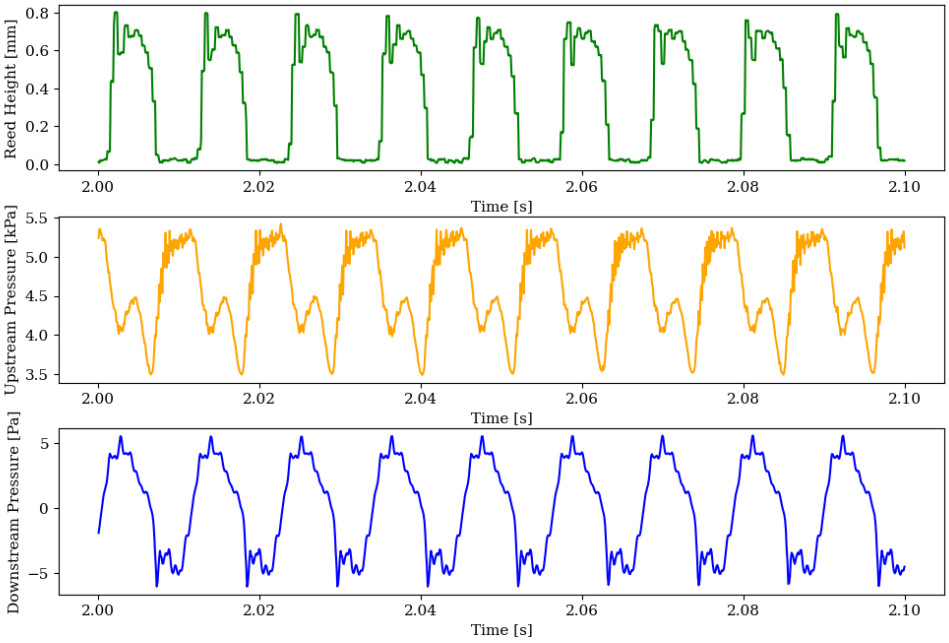

Figure 5: Measurements on the reed height, upstream, and downstream pressures for test one. The upper curve shows the reed height, with zero taken at the point of blade closure; the measurement indicates that the blades remain closed for around half of the cycle. The middle curve represents the upstream pressure, varying between 3.5 and 5.5 kPa, with a mean of approximately 4.5 kPa. The lower curve illustrates the downstream pressure, fluctuating between $\pm$ 5 kPa, with a mean of around 0 kPa.

The subsequent measurements were taken with varying blowing pressure. For tests two and three, the blowing pressure was set to the level needed for the crumhorn to produce its nominal pitch, and then it was gradually lowered until a period multiplication state emerged, considered as state B in the analysis. The last test was performed by increasing the blowing pressure from state B.

3.2 Period Multiplication Bifurcations

Period multiplication bifurcations were observed in tests two, three and four. In test two, as the blowing pressure was reduced, a quasi-stable periodic state was obtained at approximately 62 Hz (state B). The pitch variation is shown below,

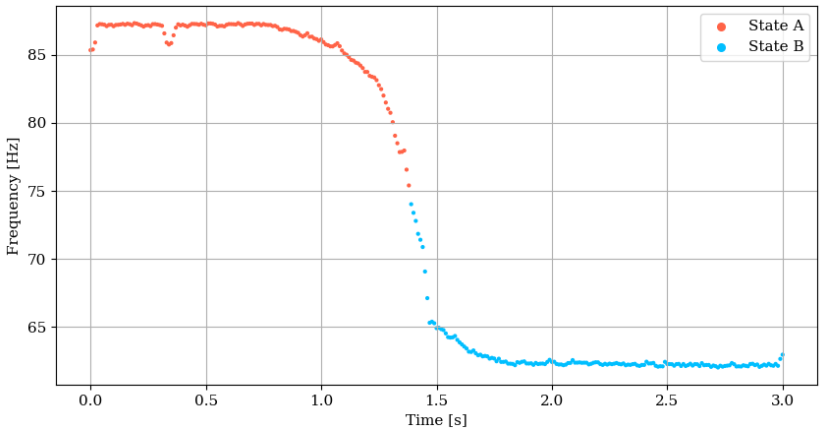

Figure 6: Pitch variation in test two as blowing pressure is reduced.

The waveforms of each stable state were measured, revealing notable differences in the downstream pressure, as shown in Figure 7. While the waveform of the downstream pressure in state B shares some qualitative similarities with state A, it is distinct in having a longer period. However, this difference does not correspond to the period doubling observed in other studies.[4] Therefore, state B may originate from a complex interaction between state A and an upper harmonic from the resonator. Models have been developed considering two quasi-harmonic resonance frequencies,[7] which describe period doubling but fail to describe these observations. A model with higher degrees of freedom may be required to describe the phenomenon.

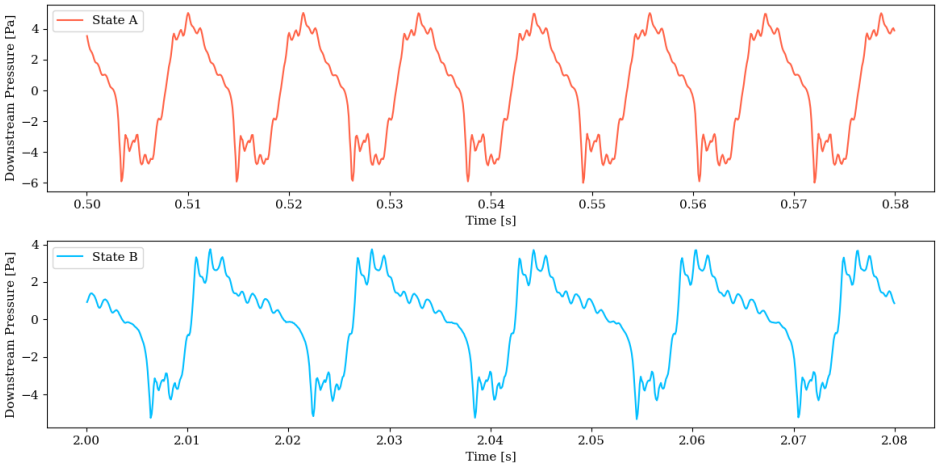

Figure 7: Downstream pressure waveform in test two of states A and B.

The same procedure was followed for tests three and four. By decreasing the speed at which the blowing pressure is reduced, a transition state (state T) between states A and B was observed in test three at an approximate frequency of 33 Hz, shown at the top of Figure 9. Generally, the T state is seen to be very unstable as the blowing pressure is reduced from state A. In the fourth test, the blowing pressure was gradually increased over an extended period. Starting from state B, the pressure was slowly raised until state A was reestablished, as illustrated at the bottom of Figure 9. In contrast with the previous test, the T state was found to be stable over a few seconds until the blowing pressure exceeds the equilibrium stability point. As in test two, Figure 8 shows that states A and B waveforms are qualitatively the same, which is expected. Remarkably, the waveform of the transition state can be seen to follow an alternation of the waveforms observed in states A and B, yielding a much longer period. This result explains the T state's low frequency measurement.

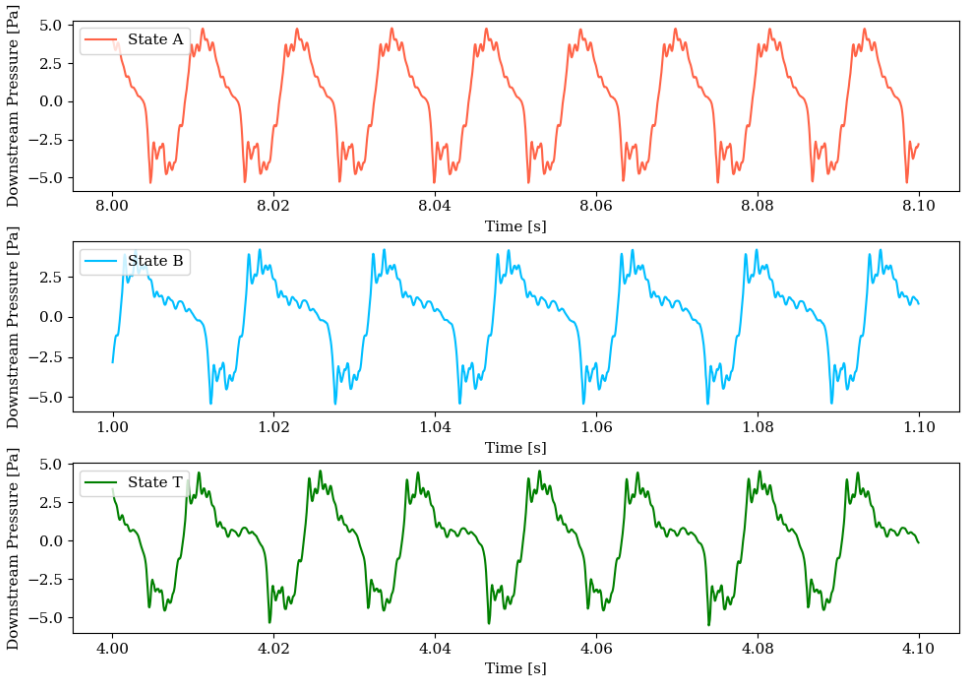

Figure 8: Downstream pressure waveform in test four of states A, B and T.

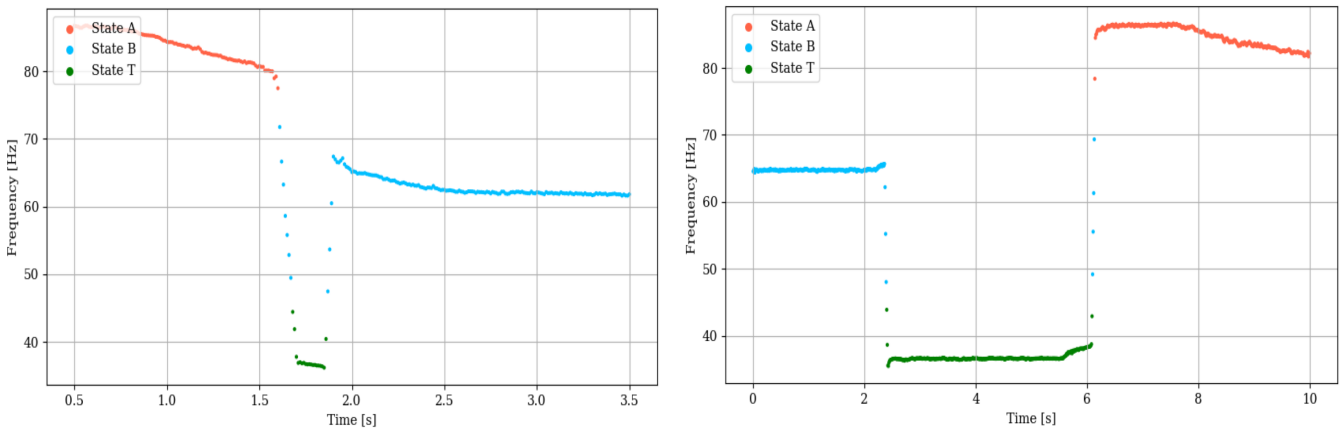

Figure 9: Left: Pitch variation in test three as blowing pressure is reduced from state A. Right: Pitch variation in test four as blowing pressure is increased from state B.

3.3 Measuring the Natural Frequency of the Reed

In addition, damped rapid oscillations appear at the maximum of the waveform of the reed blades as the F2 pitch was played, as observed in the upper plot in Figure 5. These oscillations can be directly related to the natural frequency of the reed. It was found that the high-speed camera provided more accurate measurements of these rapid oscillations compared to the laser sensor, as the laser sensor's response time was too slow to capture the full waveform. Specifically, the average response time of the laser sensor was calculated to be approximately 0.4 ms, which is insufficient for properly sampling the rapid oscillations. Figure 10 shows a comparison between the camera and laser sensor measurements, highlighting the limitations of the laser sensor in capturing these oscillations.

The high-speed camera recorded the reed's vibrations at a sample rate of 5000 frames per second. For each frame, as shown in Figure 3, a thin vertical slice of 3 pixels was taken, showing the height of both reed blades at that time. Joining all slices into a single image effectively represents the reed vibrations (Figure 10). The pixel-to-length calibration conversion is obtained by dividing the maximum oscillation measured at the laser sensor, in millimetres, by the maximum measured from the camera, in pixels. This conversion is found at 0.8276 mm. The pixel values are obtained from the image by selecting the brightest pixel at each vertical slice. This process was repeated over four periods of the reed waveform. The mean values and errors for each height value of the reed blade are obtained by selecting only the sections where rapid oscillations were observed in each period. The data is fitted to a damped sinusoidal function using a non-linear least squares minimisation. The parameters included in the fitting are the amplitude, the angular frequency of the reed and the damping constant.

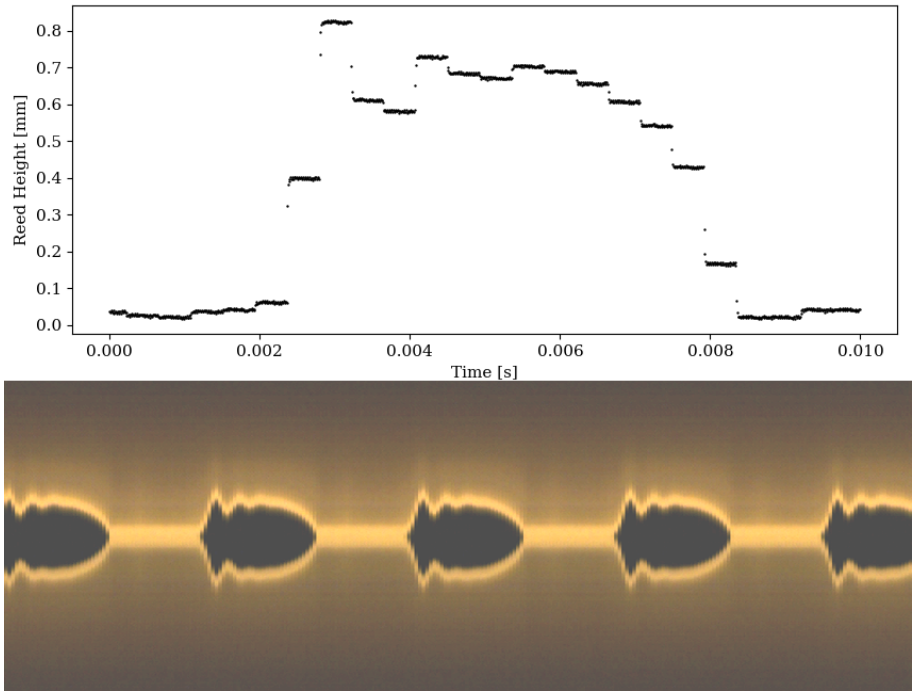

Figure 10: Top: reed height oscillations measured with the laser sensor at maximum response time. Bottom: vertical slices for each frame joined in the horizontal direction showing the reed oscillation as a function of time. The brightness and contrast have been adjusted to improve visibility.

Taking the maximum opening of the reed blade to be constant throughout the rapid oscillation, the data is centred over the average maximum of the reed opening when oscillating at the nominal pitch frequency. Fitting a damped sinusoidal function to the data yields 0.15(2) mm, 251(4) Hz and 177(34) kg/s for the amplitude, frequency and damping constant, respectively. The fitting uses a least square minimisation algorithm from the Python package `scipy.optimize`. The results are shown in Figure

11.

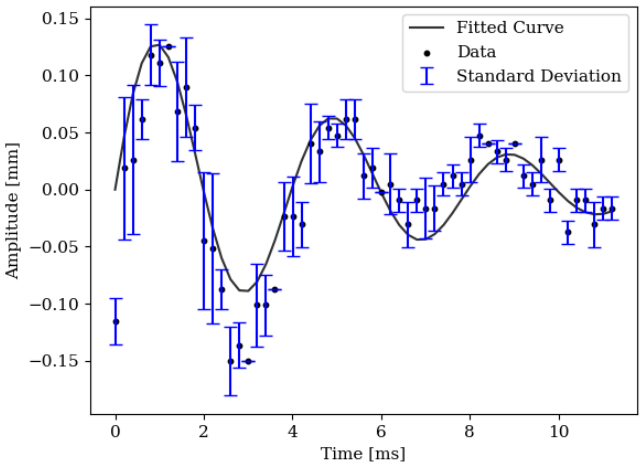

Figure 11: Rapid oscillations observed at the opening of reed blades as F2 pitch is played. Data is centred at an average oscillation value, where negative distances indicate oscillations below the average reed displacement

Comparing this result with J. Backus's experiment on clarinet reeds, which found natural frequencies of 2-3 kHz,[8] it is evident that the natural frequency obtained for the crumhorn double reed is lower. Nonetheless, the clarinet reed is considerably narrower and thinner than the double reed used in this experiment, which leads to a higher natural frequency. Moreover, the natural frequency of the reed is found well above the highest pitch played on the crumhorn, which is expected for high natural frequencies.

4 CONCLUSIONS

The period multiplication behaviour on the crumhorn matches the expected behaviour from the theoretical predictions for inverse bifurcations. However, period doubling was not obtained as the B state had a considerably larger frequency than half the frequency of the F2 pitch, which indicates that models with more than one degree of freedom may be required to represent the phenomenon. Furthermore, a transition state arises when moving between states A and B, with a waveform formed by alternating between the downstream pressure waveforms from states A and B. The alternation is observed to be quasi-periodic. The origin of the T state could also be from the Hopf bifurcation, representing another manifestation of it.

A simulation based on only one mode of the input impedance of a cylinder[9] reproduces to a reasonable extent the T state, agreeing with the alternating waveform observed. Furthermore, many more period multiplication states are possible over the Hopf bifurcation in the simulation.

5 ACKNOWLEDGEMENTS

Part of the work described in this paper was carried out by the first author as a Senior Honours Physics Project at the University of Edinburgh. The authors are grateful to Dr Sylvain Maugeais, University of Le Mans, for helpful discussions and advice on the theory of bifurcations in double reed instruments.

6 REFERENCES

[1] M. Campbell, C. Greated, A. Myers, ”Musical Instruments: History, Technology, and Performance of Instruments of Western Music”, Oxford University Press. (2004).

[2] A. Almeida, ”The Physics of Double-reed Instruments and its Application to Sound Synthesis”, PhD thesis, Univ. Pierre et Marie Curie, Paris. (2006).

[3] A. Almeida, C. Vergez, R. Caussé, and X. Rodet, “Experimental research on double reed physical properties”, Doctoral thesis, Proceedings of the Stockholm Music Acoustics Conference, Stockholm, 6. (2003).

[4] V. Gibiat, M. Castellengo, ”Period doubling occurrences in wind instruments musical performance”, Acta Acustica united with Acustica, 86(4), 746-756. (2000).

[5] A. Barjau, V. Gibiat, ”Small-Vibration Theory of the Clarinet”, J. Acoust. Soc. Am., 35(3), 305–313. (1963).

[6] J. W. Kim, J. Salamon, P. Li, J. P. Bello, ”CREPE: A Convolutional Representation for Pitch Estimation”, 2018 IEEE International Conference on Acoustics, Speech, and Signal Processing, ICASSP 2018 - Proceedings, 161-165. (2018).

[7] J. Gilbert, S. Maugeais, C. Vergez, ”From the bifurcation diagrams to the ease of playing of reed musical instruments. A theoretical illustration of the Bouasse-Benade prescription?”, Proceedings of ISMA 2019 International Symposium on Music Acoustics. (2019).

[8] J. Backus, ”Vibrations of the reed and air column in the clarinet”, J. Acoust. Soc. Am., 33(6), 806–809. (1961).

[9] S. Maugeais, ”Period doubling”, email correspondence. Email to M. G. Aragó Bishop. (2023).